Epilepsy & Behavior 99 (2019) 106455

Contents lists available at ScienceDirect

Epilepsy & Behavior

journal homepage: www.elsevier.com/locate/yebeh

A model for visual naming based on spatiotemporal dynamics of ECoG high-gamma modulation

Ravindra Arya [a,b,*,1], Abbas Babajani-Feremi [c,d,e,1], Anna W. Byars [a], Jennifer Vannest [b,f], Hansel M. Greiner [a,b], James W. Wheless [c,d], Francesco T. Mangano [g], Katherine D. Holland [a,b]

[a] Comprehensive Epilepsy Center, Division of Neurology, Cincinnati Children's Hospital Medical Center, Cincinnati, OH, United States of America
[b] Department of Pediatrics, University of Cincinnati College of Medicine, Cincinnati, OH, United States of America
[c] Department of Pediatrics, The University of Tennessee Health Science Center, Memphis, TN, United States of America
[d] Neuroscience Institute, Le Bonheur Children's Hospital, Memphis, TN, United States of America
[e] Department of Anatomy and Neurobiology, The University of Tennessee Health Science Center, Memphis, TN, United States of America
[f] Pediatric Neuroimaging Research Consortium, Cincinnati Children's Hospital Medical Center, Cincinnati, OH, United States of America
[g] Division of Pediatric Neurosurgery, Cincinnati Children's Hospital Medical Center, Cincinnati, OH, United States of America

ARTICLE INFO

Article history:
Received 10 July 2019
Revised 22 July 2019
Accepted 26 July 2019
Available online 13 August 2019

Keywords:
Presurgical language mapping
Human brain mapping
Epilepsy surgery
Neuropsychological deficits

ABSTRACT

Objective: We studied spatiotemporal dynamics of electrocorticographic (ECoG) high-gamma modulation (HGM) during visual naming.
Methods: In 8 patients, aged 4–19 years, with left hemisphere subdural electrodes, propagation of ECoG HGM during overt visual naming was mapped with trial-averaged time-frequency analysis. Group-level synthesis was performed by transforming all electrodes to a standard space and assigning cortical parcels based on a reference atlas.
Results: After image display following cortical parcels were activated: inferior occipital, caudal angular, fusiform, and middle temporal gyri, and superior temporal sulcus [0–400 ms]; rostral pars triangularis (A45r), inferior frontal sulcus, caudal dorsolateral premotor cortex (A6cdl) [300–600 ms]; caudal ventrolateral premotor cortex (A6cvl), caudal pars triangularis (A45c), pars opercularis (A44) [400–800 ms]; primary sensorimotor cortex [600–1400 ms], with most prominent HGM in glossolaryngeal region (A4tl). Lastly, auditory cortex (A41/A42) and superior temporal gyrus (A22) were activated [900 ms–1.4 s]. After 1.5 s, HGM decreased globally, except in ventrolateral premotor cortex.
Conclusions: During visual naming, ECoG HGM shows a sequential but overlapping spatiotemporal course through cortical regions. We provide neurophysiologic validation for a model of visual naming incorporating both modular and distributed cortical processing. This may explain cognitive deficits seen in some patients after surgery involving HGM naming sites outside perisylvian language cortex.

1. Introduction

Presurgical mapping of language cortex in patients with drug-resistant epilepsy (DRE) often relies on visual naming [1]. Even something seemingly as mundane as naming an image of an everyday object involves multiple cognitive domains. Different models have been proposed to explain naming function and dysfunction, including sequential and parallel processing models [1,2]. However, these models represent predominantly theoretical constructs, only partially supported by lesion or functional studies, and have scant neurophysiologic validation [2]. In patients undergoing extraoperative electrocorticographic (ECoG) monitoring, task-associated high-gamma modulation (HGM) has been shown to be a biomarker for transient speech deficits produced by electrical cortical stimulation mapping (ESM), blood-oxygen-level-dependent responses, and neuronal population firing rates [3,4]. Unlike the binary results from conventional ESM, ECoG HGM can be harnessed with sufficient spatial and temporal resolution to examine dynamic properties of cortical regions involved in visual naming. Activation of these cortical sites, particularly those outside the canonical perisylvian language cortex, may perhaps explain language and other higher-order cognitive deficits seen in DRE patients after resection of ECoG HGM language sites, which were not anticipated by the ESM [5–9]. Hence, we investigated propagation of ECoG HGM during a visual naming task to delineate cortical spatiotemporal dynamics. We

* Corresponding author at: Division of Neurology, Cincinnati Children's Hospital Medical Center, MLC 2015, 3333 Burnet Avenue, Cincinnati, OH 45229, United States of America.
E-mail address: Ravindra.Arya@cchmc.org (R. Arya).
[1] These authors contributed equally to the manuscript.

https://doi.org/10.1016/j.yebeh.2019.106455
1525-5050/

hypothesized this would show a more extensive map of cortical regions involved in language processing, perhaps explaining postoperative language deficits seen in patients with resections outside the canonical language areas and/or ESM naming sites.

2. Methods

2.1. Participants

Patients with DRE with subdural electrodes implanted over the left hemisphere, who were successfully able to complete the visual naming task, were included. These patients, recruited from Cincinnati Children's Hospital, represent a subset of those reported earlier in a study validating ECoG HGM during the naming task with ESM [10]. The present analyses were limited to patients with left hemisphere electrodes, due to better diagnostic validity of ECoG HGM for language sites in such patients. The study was approved by the Institutional Review Board of Cincinnati Children's Hospital Medical Center (#2012-0791).

2.2. ECoG signal acquisition and the naming task

Subdural electrodes used for recording ECoG signals had the following dimensions: 4.75-mm total diameter, 1.5-mm exposed diameter, and 10-mm center-to-center distance (Auragen, Integra Neurosciences, Plainsboro, NJ). For clinical purposes, extraoperative ECoG was recorded using XLTek EMU128FS amplifier (Natus Medical Inc., San Carlos, CA). For research purposes, we split signals from this amplifier into a g. USBamp (g.TEC Medical Engineering, Austria) amplifier having a sampling rate of 1.2 kHz. After obtaining a baseline with the patient silent and awake, s/he was shown a series of pictures on a monitor and requested to name them aloud. Each image display lasted 3500 ms with a 2500-ms interstimulus interval, for a total of 50 trials. Onsets and terminations of image displays were input as digital pulses time-synchronized to the ECoG data stream. Additional details about the language task, ESM, and ECoG signal acquisition have been published earlier [10].

2.3. ECoG signal processing and statistical analysis for HGM

We used similar methods for preprocessing, time-frequency analysis, and statistical analysis of ECoG signals as published previously [11,12]. After discarding electrodes with artifact or frequent epileptiform discharges and re-referencing to the grand mean, ECoG signals were converted into epoch data containing trials of the object naming task, where $t = 0$ corresponded to the onset of image display. These epoched ECoG data were then analyzed in the time-frequency domain using the multitaper method [13]. Mean power of each time-frequency bin after image display was compared to that 100 ms to 500 ms before the onset of the pictures, to calculate a t-value across all trials (separately for each electrode in every patient). The statistical significance of each time-frequency bin was determined by a Monte Carlo permutation test ($n = 10{,}000$), and significant bins ($p < 0.05$, Bonferroni corrected) were identified. We applied a 10-Hz spectral smoothing on significant time-frequency bins, and then calculated averaged 60- to 110-Hz HGM for each time bin, separately for each electrode. Although we have used the term HGM, we effectively computed power augmentation in the 60- to 110-Hz band.

2.4. Normalization and cortical parcels for subdural electrodes

To perform group-level analysis across all patients, we calculated locations of the subdural electrodes in the Montreal Neurological Institute (MNI) space using the methods described previously [11]. The postimplantation computed tomographic images of each patient were coregistered to the preimplantation magnetic resonance imaging (MRI), and locations of the subdural electrodes were extracted. We then compensated for the postsurgical brain shift, normalized the preimplantation MRI, and calculated the coordinates of the electrodes in the MNI space. We used the human Brainnetome Atlas for brain parcellation [14]. This atlas provides fine-grained brain parcellation consisting of 210 cortical and 36 subcortical regions. After normalization of the coordinates of all electrodes in all patients, electrodes with significant HGM were assigned to their nearest parcels in the Brainnetome

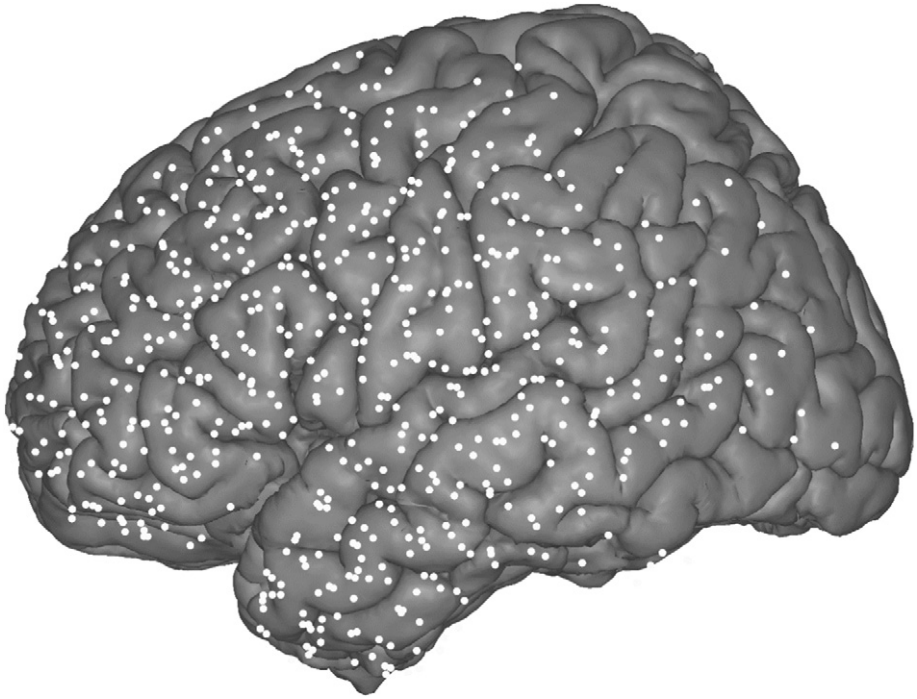

Fig. 1. Locations of the subdural electrodes of all patients are shown on the brain surface in the Montreal Neurological Institute (MNI) standard space.

atlas. Then the average time course of HGM across all significant electrodes within a parcel was calculated.

3. Results

3.1. Clinical features

Eight patients (4 females) aged 4–19 years (mean ± standard deviation 10.9 ± 4.3) were included. All the patients were native English speakers. Four patients had nonspecific findings on brain MRI, which were not useful for surgical planning, while two patients had tumors, and one each had tuberous sclerosis and periventricular heterotopia. Two of the patients were left-handed, while all others were right-handed. Functional MRI showed left language lateralization in three patients, atypical distribution (frontotemporal discordance) in one patient, and could not be performed in four patients due to inability to participate. The number of subdural electrodes varied from 58 to 126 (93 ± 23). The locations of subdural electrodes for all patients in MNI coordinates are shown in Fig. 1. Also, all cortical parcels with at least one electrode having significant HGM are shown in Fig. 2. Additional details regarding these patients have been published earlier [10].

3.2. Progression of HGM during visual naming

The mean latency of speech onset after image display was 860 ms (±49). The sequential time course of maximal high-gamma activation of cortical parcels after image display is shown in Fig. 3 for all patients. High-gamma modulation activation first started in the inferior occipital gyrus (IOG) followed by the visual area of the middle temporal gyrus (MTG) and caudal part of the angular gyrus (A39c). After approximately 400 ms poststimulus, the lateroventral and dorsolateral parts of fusiform gyrus were activated followed by the rostral and caudal parts of MTG and the anterior superior temporal sulcus (STS). Then, the inferior frontal regions and premotor cortex were activated in the following order: the rostral part of pars triangularis (A45r), inferior frontal sulcus (IFS), and the caudal dorsolateral part of premotor cortex (A6cdl). After approximately 600 ms poststimulus, the caudal ventrolateral part of premotor cortex (A6cvl) was activated followed by the caudal part of pars triangularis (A45c) and then the dorsal and ventral parts of pars opercularis (A44d and A44v). Also, although we did not observe any significant HGM in the caudal part of supramarginal gyrus (SMG; A40c), the rostrodorsal part of SMG (A40rd) was activated approximately 700 ms after stimulus onset. After that, the primary motor and somatosensory cortices were activated. The most prominent HGM was seen in the tongue and larynx region of motor cortex (A4tl). Finally, the auditory cortex (A41/A42) was activated followed by the caudal and rostral parts of superior temporal gyrus (STG; A22c and A22r). After 1.5 s of visual stimulus, HGM decreased in all areas, but ventrolateral premotor cortex continued to maintain activation.

4. Discussion

4.1. Neurophysiology of dynamic localization of ECoG HGM during visual naming

This study showed temporal dynamic localization of ECoG HGM during visual naming to different cortical areas. While conventional ESM offers only binary classification of cortical sites into those with and without speech arrest, our study provides neurophysiologic evidence for different cognitive components involved in visual naming. The initial HGM was localized to IOG, visual area in the MTG, and caudal angular gyrus (A39c), attesting to their role in the initial decoding of the graphic information from the displayed image. Within the next 400 ms, fusiform

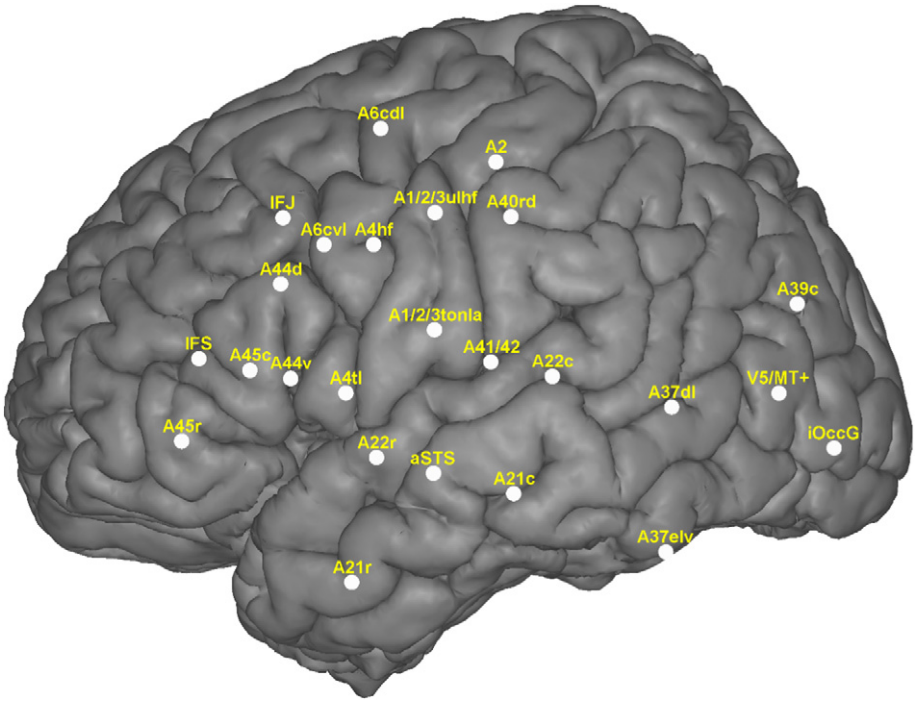

Fig. 2. Cortical parcels with significant high-gamma modulation in the human Brainnetome atlas. A1/2/3 tonla: Area 1/2/3 (tongue and larynx); A1/2/3 ulhf: Area 1/2/3 (upper limb, head, and face); A2: Area 2; A4hf: Area 4 (head and face); A4tl: Area 4 (tongue and larynx); A6cdl: caudal dorsolateral Area 6 (Premotor cortex); A6cvl: caudal ventrolateral Area 6 (Premotor cortex); A21c: caudal Area 21 (Middle Temporal Gyrus, MTG); A21r: rostral Area 21 (MTG); A22c: caudal Area 22 (STG); A22r: rostral Area 22 (Superior Temporal Gyrus, STG); A37dl: dorsolateral Area 37 (Fusiform gyrus); A37elv: extreme lateroventral Area 37 (Fusiform gyrus); A39c: caudal Area 39 (Angular gyrus); A40rd, rostrodorsal Area 40 (Supra-marginal gyrus); A41/42: Area 41/42 (Auditory cortex); A44d: dorsal Area 44 (Pars opercularis); A44v: ventral Area 44 (Pars opercularis); A45c: caudal Area 45 (Pars triangularis); A45r: rostral Area 45 (Pars triangularis); ASTS: anterior superior temporal sulcus; IFJ: inferior frontal junction; IFS: inferior frontal sulcus; iOccG: inferior occipital gyrus; V5/MT+: the middle temporal visual area.

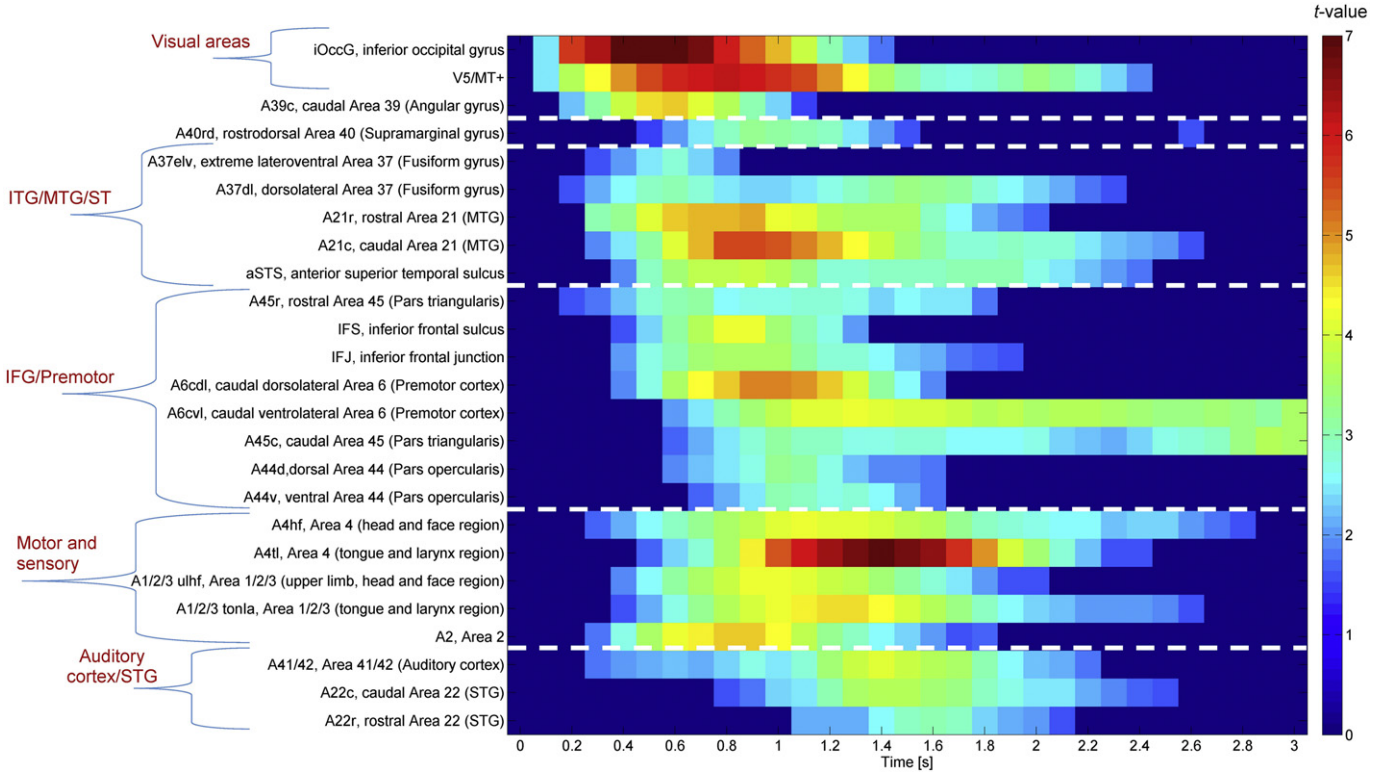

Fig. 3. Time courses of maximal high-gamma augmentation in different cortical parcels during overt picture naming (data from all patients). Time 0 corresponds to onsets of image displays. Color bar represents *t*-value of high-gamma augmentation for each electrode with respect to its baseline (100–500 ms before picture display). See Fig. 2 for the locations of the cortical areas in the MNI atlas.

gyrus, MTG, and STS were activated, suggestive of interpretation of the substantive content of the image and lexical access. Certain regions in the inferior frontal lobe were next to show HGM including rostral pars triangularis, IFS, and caudal dorsolateral premotor cortex. Notably, there is overlap between the poststimulus time-course for activation of Broca's and Wernicke's areas, suggesting bidirectional information sharing in the perisylvian cortex, rather than sequential transfer [15]. About 600 ms after the image display, HGM was noted in caudal ventrolateral premotor cortex, caudal pars triangularis (A45c) and pars opercularis (A44). This activation in Broca's area likely represents binding the semantic and lexical representations of the visual content to the articulatory representation of the spoken word, which is then passed on to motor areas for speech, as seen by subsequent activation of the primary sensorimotor cortex [16]. The most prominent HGM was indeed seen in the glossolaryngeal representation (A4tl). Lastly, the auditory cortex (A41/A42) along with STG showed HGM, likely related to awareness and monitoring of the self-voice [17]. After 1.5 s of visual stimulus, HGM decreased in all areas, though ventrolateral premotor cortex continued to show activation, probably suggesting a role in sustaining attention during and after the language task.

4.2. Spatiotemporally distributed model for visual naming

Our observations allow us to propose a model for the functional neuroanatomy of visual naming (Table 1). We propose that visual naming involves 5 phases, having overlapping poststimulus time courses, with distributed topography of HGM and corresponding physiology. As a perspective, previous models to explain language processing in the brain

Table 1
Proposed neurophysiological model for visual naming based on propagation of electrocorticographic high-gamma modulation.

Phase	Poststimulus time	Localization of high-gamma modulation	Probable neurophysiologic role
Visual Decoding	0–400 ms	1.1: Inferior occipital gyrus, followed by the middle temporal visual area, and caudal part of angular gyrus 1.2: Ventrolateral and dorsolateral parts of fusiform gyrus, rostral and caudal parts of the middle temporal gyrus, and anterior superior temporal sulcus	Decoding of graphic information in the image Contextual interpretation of graphic content (visual association cortex)
Semantic-Lexical	300–600 ms	2.1: Rostral part of pars triangularis 2.2: Inferior frontal sulcus, and caudal dorsolateral premotor cortex	Extraction of meanings (semantics) and word representations (lexicon) from the graphic content
Phonemic	400–800 ms	3.1: Caudal ventrolateral part of premotor cortex 3.2: Caudal part of pars triangularis 3.3: Dorsal and ventral parts of pars opercularis	Correlating extracted word representations to appropriate sound sequences (phonemes) for verbal expression Motor program generation
Articulatory	600 ms–1.4 s	4.1: Primary sensorimotor cortex (most prominent HGM in tongue and laryngeal region)	Executing the motor speech program Verbal expression and articulation
Modulation	1.2–1.8 s	5.1: Auditory cortex 5.2: Superior temporal gyrus	Feedback cross-checking and self-voice modulation

have included neurological, cognitive, and connectionist models [18]. These models have described both modular and distributed processing, and were based mostly on lesion–symptom correspondence and neuropsychological data. However, these models were not constrained by neurophysiology and have only limited support from functional imaging [19]. For example, functional data has highlighted the role of angular gyrus in semantic decision making, and that of posterior inferior temporal lobe in orthographic interpretation and name retrieval, which were missing from the lesion-based models [18,20]. The dual-stream models based on functional imaging propose initial phonological analysis in STG and STS, and subsequent branching into concurrent ventral stream through anterior and middle temporal lobe for speech recognition and lexical representation, and dorsal stream including dominant posterior frontal lobe, perirolandic cortex, and dorsal STG, responsible for phonetic and articulatory processing [21,22]. There is disagreement between the two main dual-stream models regarding bilateral versus dominant hemisphere processing of speech perception. These concepts were extended by the hodotopical (delocalized) model, which proposed that following the visual input, the language network is organized in parallel distinct, but interconnected, corticosubcortical subnetworks underlying semantic, phonological, and syntactic processing [23].

Our model incorporates elements of both modular and parallel processing, and proposes that individual elements of graphic, contextual, semantic, lexical, and phonological processing may proceed concurrently, with overlapping but staggered time courses, eventually culminating into articulation and feedback self-modulation. We believe that we add two aspects to the existing models. First, we provide direct neurophysiologic evidence for our model, and secondly, add a temporal dimension to the subcomponents. However, our model is limited to overt picture naming and does not address other aspects of language processing in the brain [5,24–26]. This is important because in a study including 8 patients with DRE, perisylvian activations seen early in the perceptual phase of a word-repetition task, were maintained through overt articulation, but attenuated during covert expression [27]. Authors inferred that perisylvian speech network is modulated by the demands of different conditions. This task-specificity of HGM topography was also shown in another study including 79 patients, where picture naming elicited HGM preferentially medial to left inferior temporal gyrus, while auditory naming elicited HGM more laterally, before response onset, although inferior precentral HGM was seen immediately after stimulus onset with both tasks [28]. Also, we did not observe significant HGM in the caudal SMG, compared to the hodotopical model [23]. We suspect that this could be due to our observations being based on a single task, compared to a synthesis of data from several language tasks in the other models [1].

Our findings are aligned with, but more detailed than, previous ECoG studies. In seven adults, a study showed different temporal envelopes for HGM in cortical language networks, resulting in complex, cascading spatiotemporal patterns of activation [29]. During object naming, sequential HGM was noted in basal temporal-occipital cortex (visual processing), followed by Broca's area and sensorimotor cortex (speech planning and preparation) [29]. Another large study ($n = 100$) including 16 children (<10 years of age), using an auditory naming task, found 70- to 110-Hz HGM in bilateral STG and precentral gyri immediately after question onset, and left temporal/frontal lobes, left inferior parietal, and cingulate regions, around question offset [30]. Immediately before verbal response, HGM involved bilateral posterior superior frontal, and pre-/postcentral regions [30]. Interestingly, in our study, a stronger HGM was noted in the glossolaryngeal motor cortex, compared to Broca's area. We speculate that this might represent the greater likelihood of reorganization in Broca's area in DRE compared to motor cortex, which is relatively resistant to the network plasticity from epilepsy [31,32]. Another study has also shown initial high-gamma suppression followed by augmentation in left lateral prefrontal regions including Broca's area, several hundred ms before response onset during visual and auditory naming tasks [28]. While early high-gamma suppression within Broca's area was more intense during picture naming, subsequent prefrontal high-gamma augmentation was more intense during auditory naming. Although we analyzed only power augmentation, we believe that this finding is consistent with ours, and may suggest wider generalizability [33].

4.3. Clinical significance of spatiotemporal aspects of HGM language mapping

Our observations and the proposed model generate a hypothesis for neuropsychological deficits seen in some patients after epilepsy surgery. Studies have shown cognitive deficits after cortical resections, which spared ESM naming sites but included HGM language sites. Recently, in 17 patients, we used principal component analysis of multiple neuropsychological measures to find that the first component score increased by 14 points in patients whose resections spared HGM naming sites, whereas it decreased by 8 points when the resections included HGM sites [9]. On further analysis, a significant difference of 15 points was seen in working memory between the groups of patient with/without resection of HGM visual naming sites. In another recent study, resection of HGM naming sites resulted in postoperative naming decline in 3/11 patients, although these sites were ESM negative [34]. Earlier, 7/11 adults were reported to have postoperative language deficits that were not anticipated by ESM [5]. In 4/7 of these patients, the resection included HGM naming sites, and was associated with poorer performance on Hopkins verbal learning test, poorer verbal fluency, and transcortical motor aphasia. In a study including native Dutch speakers, 2/6 patients had postoperative aphasia after resection of HGM language sites [6]. Similarly, expressive aphasia, impaired naming, and verbal memory decline have been reported in 2 other patients [7,8]. Our observations can help explain these higher-order cognitive deficits even though the ESM naming sites were spared during epilepsy surgery. We think that these deficits may result from resection of brain regions outside the conventional perisylvian language cortex, which are involved in different components of visual naming at various time points.

5. Challenges and conclusions

The limitations of our study stem mainly from the fact that we have analyzed ECoG signals. While offering excellent spatial and temporal resolution, subdural electrodes are surgically implanted for extraoperative monitoring only in patients with valid indications, most commonly DRE. Hence, our findings may not be generalizable to neurologically healthy children. Secondly, the configuration and position of subdural electrodes is individualized based on presumptive location of seizure-onset zone, and is not standardized like scalp electroencephalography (EEG). Hence, ECoG coverage is heterogeneous with variable electrode density in different cortical parcels. Our analysis was limited to patients with left hemisphere electrodes, due to our previous observation that ECoG HGM is a better predictor of ESM naming sites in the left hemisphere [10]. Thus, we could not analyze the bilateral contributions to certain phases of language processing. Also, we could not analyze the role of subcortical pathways in language processing, due to the absence of sampling from those regions. We hope to extend our methodology to stereo-EEG in near future to address these limitations.

In summary, based on analysis of ECoG HGM during a visual naming task, we have shown a sequential but overlapping cascade of activation through different cortical regions. This allowed us to propose a model for naming consisting of visual, semantic/lexical, phonological, articulatory, and self-modulation phases. While these modules are spatiotemporally distributed during the naming task, there is an ordered structure to them. This led us to speculate that perhaps language processing in the brain involves both modular and parallel processing. We were able to refine the existing models for visual naming, and provide neurophysiologic validation for the same. In future, it will be desirable to perform a similar analysis in a larger sample of patients with

bilateral electrodes including both subdural and stereotactic depth electrodes, having a wider age range, and including multiple language tasks. This will allow synthesizing a more comprehensive model for language processing in the human brain, its development with the age, and interaction with epilepsy.

Declaration of Competing Interest

This work was supported by the Cincinnati Children's Research Foundation (Research innovation project grant), Procter Foundation (Procter Scholar Award), the Division of Neurology at Cincinnati Children's Hospital Medical Center; and the Le Bonheur Children's Hospital, the Children's Foundation Research Institute, the Le Bonheur Associate Board, Memphis, TN. Funding sources had no role in study design, data acquisition, analysis, and the decision to submit the manuscript. RA receives research support from the Procter Foundation (principal investigator) and the Maxon Foundation (coinvestigator).

Appendix A. Supplementary data

Supplementary data to this article can be found online at https://doi.org/10.1016/j.yebeh.2019.106455.

References

[1] Hamberger MJ. Object naming in epilepsy and epilepsy surgery. Epilepsy Behav 2015;46:27–33.
[2] Chang EF, Raygor KP, Berger MS. Contemporary model of language organization: an overview for neurosurgeons. J Neurosurg 2015;122:250–61.
[3] Arya R, Horn PS, Crone NE. ECoG high-gamma modulation versus electrical stimulation for presurgical language mapping. Epilepsy Behav 2018;79:26–33.
[4] Lachaux JP, Fonlupt P, Kahane P, Minotti L, Hoffmann D, Bertrand O, et al. Relationship between task-related gamma oscillations and BOLD signal: new insights from combined fMRI and intracranial EEG. Hum Brain Mapp 2007;28:1368–75.
[5] Cervenka MC, Corines J, Boatman-Reich DF, Eloyan A, Sheng X, Franaszczuk PJ, et al. Electrocorticographic functional mapping identifies human cortex critical for auditory and visual naming. Neuroimage 2013;69:267–76.
[6] Bauer PR, Vansteensel MJ, Bleichner MG, Hermes D, Ferrier CH, Aarnoutse EJ, et al. Mismatch between electrocortical stimulation and electrocorticography frequency mapping of language. Brain Stimul 2013;6:524–31.
[7] Sinai A, Bowers CW, Crainiceanu CM, Boatman D, Gordon B, Lesser RP, et al. Electrocorticographic high gamma activity versus electrical cortical stimulation mapping of naming. Brain 2005;128:1556–70.
[8] Kojima K, Brown EC, Rothermel R, Carlson A, Matsuzaki N, Shah A, et al. Multimodality language mapping in patients with left-hemispheric language dominance on Wada test. Clin Neurophysiol 2012;123:1917–24.
[9] Arya R, Roth C, Leach JL, Middeler D, Wilson JA, Vannest J, et al. Neuropsychological outcomes after resection of cortical sites with visual naming associated electrocorticographic high-gamma modulation. Epilepsy Res 2019;151:17–23.
[10] Arya R, Wilson JA, Fujiwara H, Rozhkov L, Leach JL, Byars AW, et al. Presurgical language localization with visual naming associated ECoG high-gamma modulation in pediatric drug-resistant epilepsy. Epilepsia 2017;58:663–73.
[11] Babajani-Feremi A, Narayana S, Rezaie R, Choudhri AF, Fulton SP, Boop FA, et al. Language mapping using high gamma electrocorticography, fMRI, and TMS versus electrocortical stimulation. Clin Neurophysiol 2016;127:1822–36.
[12] Babajani-Feremi A, Rezaie R, Narayana S, Choudhri AF, Fulton SP, Boop FA, et al. Variation in the topography of the speech production cortex verified by cortical stimulation and high gamma activity. Neuroreport 2014;25:1411–7.
[13] Mitra PP, Pesaran B. Analysis of dynamic brain imaging data. Biophys J 1999;76:691–708.
[14] Fan L, Li H, Zhuo J, Zhang Y, Wang J, Chen L, et al. The human Brainnetome atlas: a new brain atlas based on connectional architecture. Cereb Cortex 2016;26:3508–26.
[15] Arya R, Ervin B, Wilson JA, Byars AW, Rozhkov L, Buroker J, et al. Development of information sharing in language neocortex in childhood-onset drug-resistant epilepsy. Epilepsia 2019;60:393–405.
[16] Middlebrooks EH, Yagmurlu K, Szaflarski JP, Rahman M, Bozkurt B. A contemporary framework of language processing in the human brain in the context of preoperative and intraoperative language mapping. Neuroradiology 2017;59:69–87.
[17] Terband H, Maassen B, Guenther FH, Brumberg J. Auditory-motor interactions in pediatric motor speech disorders: neurocomputational modeling of disordered development. J Commun Disord 2014;47:17–33.
[18] Price CJ. The anatomy of language: contributions from functional neuroimaging. J Anat 2000;197(Pt 3):335–59.
[19] Hickok G. The architecture of speech production and the role of the phoneme in speech processing. Lang Cognit Process 2014;29:2–20.
[20] Di Virgilio G, Clarke S. Direct interhemispheric visual input to human speech areas. Hum Brain Mapp 1997;5:347–54.
[21] Hickok G, Poeppel D. The cortical organization of speech processing. Nat Rev Neurosci 2007;8:393–402.
[22] Rauschecker JP, Scott SK. Maps and streams in the auditory cortex: nonhuman primates illuminate human speech processing. Nat Neurosci 2009;12:718–24.
[23] Duffau H, Moritz-Gasser S, Mandonnet E. A re-examination of neural basis of language processing: proposal of a dynamic hodotopical model from data provided by brain stimulation mapping during picture naming. Brain Lang 2014;131:1–10.
[24] Arya R, Wilson JA, Fujiwara H, Vannest J, Byars AW, Rozhkov L, et al. Electrocorticographic high-gamma modulation with passive listening paradigm for pediatric extraoperative language mapping. Epilepsia 2018;59:792–801.
[25] Arya R, Wilson JA, Vannest J, Byars AW, Greiner HM, Buroker J, et al. Electrocorticographic language mapping in children by high-gamma synchronization during spontaneous conversation: comparison with conventional electrical cortical stimulation. Epilepsy Res 2015;110:78–87.
[26] Kojima K, Brown EC, Matsuzaki N, Rothermel R, Fuerst D, Shah A, et al. Gamma activity modulated by picture and auditory naming tasks: intracranial recording in patients with focal epilepsy. Clin Neurophysiol 2013;124:1737–44.
[27] Leuthardt EC, Pei XM, Breshears J, Gaona C, Sharma M, Freudenberg Z, et al. Temporal evolution of gamma activity in human cortex during an overt and covert word repetition task. Front Hum Neurosci 2012;6:99.
[28] Nakai Y, Sugiura A, Brown EC, Sonoda M, Jeong JW, Rothermel R, et al. Four-dimensional functional cortical maps of visual and auditory language: intracranial recording. Epilepsia 2019;60:255–67.
[29] Wang Y, Fifer MS, Flinker A, Korzeniewska A, Cervenka MC, Anderson WS, et al. Spatial-temporal functional mapping of language at the bedside with electrocorticography. Neurology 2016;86:1181–9.
[30] Nakai Y, Jeong JW, Brown EC, Rothermel R, Kojima K, Kambara T, et al. Three- and four-dimensional mapping of speech and language in patients with epilepsy. Brain 2017;140:1351–70.
[31] Goldmann RE, Golby AJ. Atypical language representation in epilepsy: implications for injury-induced reorganization of brain function. Epilepsy Behav 2005;6:473–87.
[32] Baciu M, Perrone-Bertolotti M. What do patients with epilepsy tell us about language dynamics? A review of fMRI studies. Rev Neurosci 2015;26:323–41.
[33] Asano E, Brown EC, Juhasz C. How to establish causality in epilepsy surgery. Brain Dev 2013;35:706–20.
[34] Babajani-Feremi A, Holder CM, Narayana S, Fulton SP, Choudhri AF, Boop FA, et al. Predicting postoperative language outcome using presurgical fMRI, MEG, TMS, and high gamma ECoG. Clin Neurophysiol 2018;129:560–71.